Condensation of FtsZ filaments can drive bacterial cell division

Ganhui Lan[a], Brian R. Daniels[b], Terrence M. Dobrowsky[b], Denis Wirtz[b], and Sean X. Sun[a,b,c,1]

Departments of [a]Mechanical Engineering and [b]Chemical and Biomolecular Engineering and [c]Whitaker Insitute of Biomedical Engineering, The Johns Hopkins University, Baltimore, MD 21218

Edited by George Oster, University of California, Berkeley, CA, and approved November 18, 2008 (received for review August 13, 2008)

Forces are important in biological systems for accomplishing key cell functions, such as motility, organelle transport, and cell division. Currently, known force generation mechanisms typically involve motor proteins. In bacterial cells, no known motor proteins are involved in cell division. Instead, a division ring (Z-ring) consists of mostly FtsZ, FtsA, and ZipA is used to exerting a contractile force. The mechanism of force generation in bacterial cell division is unknown. Using computational modeling, we show that Z-ring formation results from the colocalization of FtsZ and FtsA mediated by the favorable alignment of FtsZ polymers. The model predicts that the Z-ring undergoes a condensation transition from a low-density state to a high-density state and generates a sufficient contractile force to achieve division. FtsZ GTP hydrolysis facilitates monomer turnover during the condensation transition, but does not directly generate forces. In vivo fluorescence measurements show that FtsZ density increases during division, in accord with model results. The mechanism is akin to van der Waals picture of gas-liquid condensation, and shows that organisms can exploit microphase transitions to generate mechanical forces.

force generation | modeling | Z-ring

Cytokinesis is the final step of cell division. For bacterial cells, FtsZ filaments and several related proteins form a contractile ring (Z-ring) and drive cytokinesis (1–3). FtsZ is a tubulin homologue that hydrolyzes GTP (4, 5), although GTP hydrolysis activity is not essential for bacterial division (6). Recently, force generation by membrane-bound FtsZ in vesicles was observed (7). Thus, the role of the Z-ring seems to be 2-fold: It recruits cell wall synthesis proteins, facilitating cell wall growth and remodeling (2, 3), and it exerts a weak mechanical force to direct cell wall growth (8). Bacterial genome does not appear to code for contractile molecular motors, thus prompting the question: what is the mechanism of Z-ring formation and ensuing force generation?

Earlier studies of FtsZ polymerization showed that FtsZ monomers can form polymer bonds and lateral bundling bonds (9–13). FtsZ forms proto-filament under low concentration and these proto-filaments interact with each other and form long but narrow bundles when FtsZ concentration is high (14). Quantitative analysis of in vitro polymerization kinetics indicated that the polymer bond is $-17 \approx -20\ k_BT$, and the lateral bond is $-0.2 \approx -0.5\ k_BT$, depending on the buffer condition (13). (k_BT is 4.2 pNnm.) A GTP hydrolysis-associated conformational change has been observed for FtsZ filaments (9). However, it can be shown that the conformational change is unlikely to generate sufficient contractile force (see *Discussion*). A different mechanism of force generation must be at play.

FtsA and ZipA are 2 proteins essential for the formation and maintenance of the Z-ring. Spatial regulation of the ring positioning is achieved in part through the action of the MinCDE system. MinC is a negative regulator of FtsZ polymerization and is a part of the MinCDE system (12). MinCDE form either an oscillatory or stationary pattern in the cell (15); the result is a low-MinC region at the mid-cell. Because MinC weakens/limits both lateral and longitudinal bonds of FtsZ, in high MinC regions, the binding energy is not sufficient to compete with the entropy of free FtsZ. Polymerization of long filaments is only favorable at the low MinC region at the mid-cell. FtsA and ZipA, which anchor their binding partners to the membrane, colocalize with FtsZ at the ring region and promote FtsZ bundling (3, 16–20) (Fig. 1*A*). To concretely understand the force generation mechanism of the Z-ring, we developed a lattice model of FtsZ dynamics (Fig. 1 *B* and *SI Text*). Our study reveals that the ring forms as a spontaneous condensation of FtsZ/FtsA driven by alignment of long polymers in the hoop direction. Z-ring contraction and force generation can be explained by a microphase transition powered by lateral interactions between FtsZ filaments.

Model and Experiment. FtsZ filaments are unstable. Rapid monomer exchange between the ring and the cytoplasm has been observed in vivo (21). The instability is directly related to the longitudinal (polymer) bond energy of the filament, e_1, which allow the filaments to break at the ends and in the middle. Filament breakage occur spontaneously without GTP hydrolysis, although GTP hydrolysis does increase the filament breakage rate (13). FtsZ filament also interact with each other laterally with bond energy e_2. Even though e_2 is significantly weaker than e_1, the total lateral interaction scales as the number of lateral contacts in the Z-ring. A more negative value of e_2 will favor higher number lateral contacts between filaments, and the overall density of FtsZ in the ring region will be high. A higher e_2 will favor smaller number of lateral contacts due to entropic expansion.

Fig. 1*A* shows a schematic of the system and the major components considered in our model. The cytoplasmic space and the inner membrane layer are divided into a lattice where FtsZ, FtsA, and ZipA can freely occupy. Formation and breakage of filaments are accounted for by allowing each lattice point to change occupancy. The overall energy of the system is computed for each configuration by summing all lateral and longitudinal interactions, and interaction with membrane bound FtsA/ZipA. The probability of changing the system configuration is governed by the energies before and after the change, according to the Metropolis criterion. Entropy of the system is also accounted for by examining the probabilities of configurations. The detailed specifications of our model are discussed in *SI Text*. By carrying out simulations according to the energetics of FtsZ interactions, it is possible to watch the system evolve to form a ring (Movie S1), examine monomer exchange (Movie S2) and compute the contraction force (Movie S3).

To see that lateral interaction can drive Z-ring contraction, a simple 1D model is illustrative (Fig. 1*C*). Two filaments are attached at opposite ends, and are slightly overlapping. The energy can be lowered in 2 ways. Scenario one is by adding a monomer to the free end of one of the filaments; the number of lateral contacts

Author contributions: D.W. and S.X.S. designed research; G.L., B.R.D., T.M.D., and S.X.S. performed research; G.L. analyzed data; and G.L., D.W., and S.X.S. wrote the paper.

The authors declare no conflict of interest.

This article is a PNAS Direct Submission.

[1]To whom correspondence should be addressed. E-mail: ssun@jhu.edu.

This article contains supporting information online at www.pnas.org/cgi/content/full/0807963106/DCSupplemental.

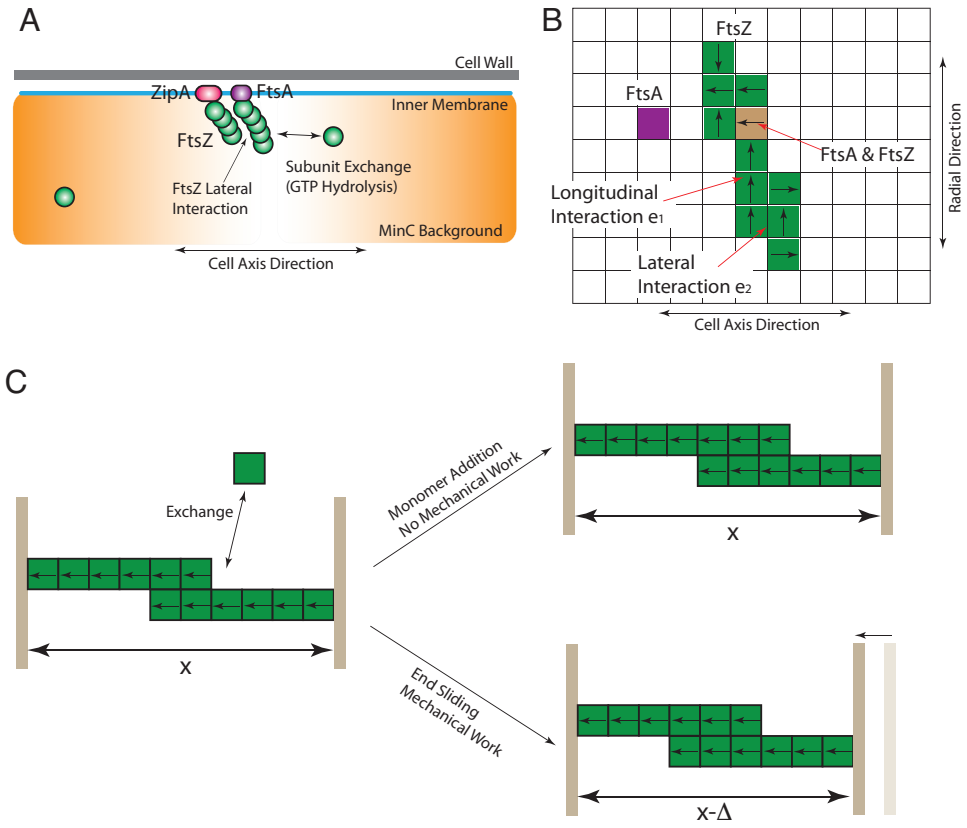

Fig. 1. Lattice model of the Z-ring. (*A*) A schematic of the Z-ring, which contains FtsA/ZipA interacting with FtsZ in a nonuniform MinC background. A gradient in MinC (orange) allows FtsA/ZipA to colocalized with FtsZ. (*B*) A lattice representation of FtsZ interaction. Each lattice can be either empty or filled with FtsZ, FtsA, or FtsZ+FtsA. FtsZ can either orient in the cell-axis direction or the hoop direction. Two FtsZ molecules end-to-end have a longitudinal interaction (polymer bond) energy e_1. Two parallel FtsZ side-to-side have a lateral interaction energy e_2. All other adjacent orientations do not interact. (*C*) The basic force generation mechanism is by increasing the number of lateral contacts between filaments. Increasing the number of lateral contacts, which can occur by adding a monomer or sliding the filament end, lowers energy. The probability of adding a monomer is controlled by the cytoplasmic concentration. The sliding of the filament end performs mechanical work. Our model reveals that the second scenario is most probable and is the force generation mechanism.

and polymer bonds are increased by one. Scenario two is to move the attachment by a distance of 1 monomer; the number of lateral contacts is again increased by 1, but the number of polymer bonds remains the same. The second scenario also has generated a contractile force of e_2/Δ, where $\Delta = 5$ nm is the monomer size. When summed over many interacting filaments, a significant contractile force can be achieved (see *Results*). In the actual system, both scenarios are happening. However, the probability of the second scenario is much higher because the addition of a monomer is controlled by the available free monomers in the cytoplasm. Under normal FtsZ expression levels, the number of free monomers in the cytoplasm is maintained such that the scenario two is primary mechanism of increasing FtsZ density in the Z-ring (see *Results*).

The model predicts that FtsZ density in the ring region should increase as the cell contracts. To check the model predictions, we obtained fluorescent images of FtsZ::GFP expressing bacteria. Three-dimensional timelapse images were acquired and analyzed to obtain the total fluorescent intensity, and intensity density in the ring area. The image analysis details are given in *SI Text*.

Results

Z-Ring Formation. Before *Escherichia coli* divides, $\approx 10^4$ FtsZ particles (7 μM) are in the cytoplasm and 700 FtsA and 1,500 ZipA are randomly distributed on the membrane (22). FtsZ can bind both FtsA and ZipA (19). Live cell microscopy suggests that FtsZ form polymers, and become anchored to the membrane when it binds FtsA/ZipA (23). However, interaction of FtsZ with MinC reduces the length of FtsZ filaments (12). Our Monte Carlo simulation shows that, in the presence of a MinC gradient, long FtsZ filaments can only grow in the low MinC region. Simulations also reveal how FtsZ colocalizes with FtsA/ZipA and the formation of an initially disordered Z-ring (Fig. 1*C* and Movie S1). As the ring forms, FtsA and ZipA are attracted to the dense FtsZ region and eventually are completely confined to the ring.

To form a ring, most of the FtsZ filaments must align and extend in the hoop direction at the division site. Our model explains this from an energetic point of view. In vitro polymerization analysis has shown that FtsZ monomers in polymers can interact with each other through longitudinal and lateral bonds (13). The longitudinal (polymer) bond energy, $e_1 = -17\ k_BT$, is much larger than the lateral bond energy, $e_2 = -0.2\ k_BT$ (13). GTP hydrolysis mediates the breakage of longitudinal bonds. In the lattice model, we incorporate FtsZ–FtsZ interactions according to the estimated bond energies. As the system evolves toward a steady state, 90% of the filaments eventually become oriented in the hoop direction (see *SI Text*). Numerical simulation shows that 2500 FtsZ molecules and almost all FtsA+ZipA occupy 30% of the membrane area in the low MinC region. In many places, there are empty voids and the ring is not fully connected around the cell circumference. However, the ring is dynamic and filaments constantly fluctuate. At steady state, we find a continuous exchange of FtsZ between the ring and the cytoplasm, in agreement with previous FRAP study results (21) (Movie S2). There are 90 filaments in the ring with lengths between 15 and 450 nm. The average length is 127 nm.

Z-ring Contraction. Other division proteins can regulate the interaction between FtsZ laments (18), a yet unidentified signal causes the Z-ring to contract. We postulate that the signal enhances lateral interaction energy between FtsZ, and model this effect by increasing e_2. The ring spontaneously undergoes a transition from the initial low-density state toward a high-density state (Movie S3). Now, attractions between FtsZ are able to out-compete entropic effects and the density in the ring increases. A priori, FtsZ density could increase by either increasing the number of FtsZ monomers in the Z-ring or decreasing the area where the ring resides by decreasing the ring radius. The ring radius can decrease via the

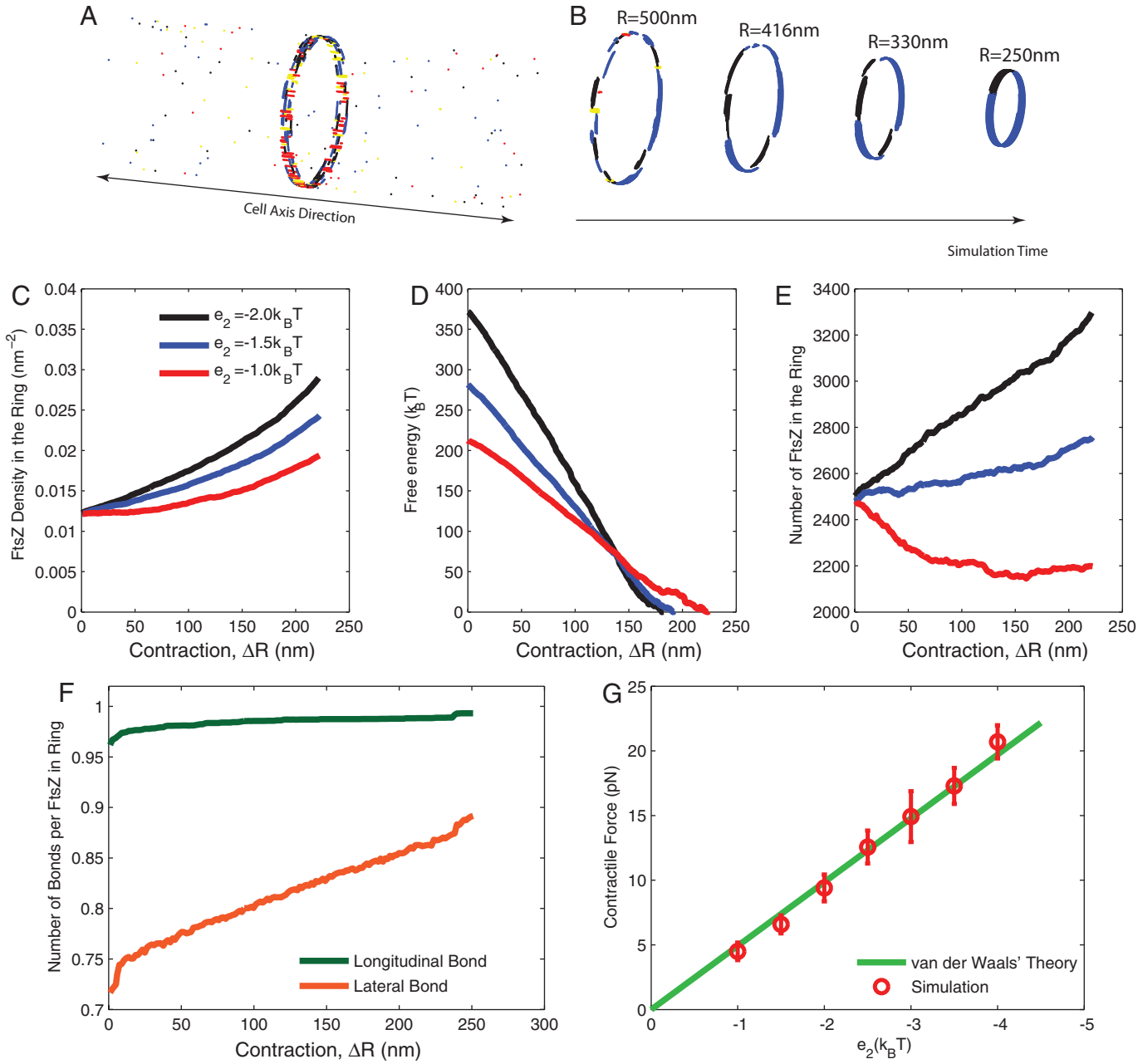

Fig. 2. Model results. (*A*) Snapshot of a nascent Z-ring with a weak lateral interaction e_2. The filaments are short and disordered, and can orient in any direction. Red and yellow correspond to parallel and anti-parallel to the cell-axis, respectively. Blue and black correspond to clockwise and counterclockwise filament orientation in the hoop direction. (*B*) Series of configurations during Z-ring contraction. Filaments during this stage become longer and more aligned in the hoop direction. (*C*) During contraction, the number density of FtsZ in the ring region increases. (*D*) The free energy of the ring decreases with decreasing ring radius, suggesting that there is a thermodynamic contractile force given by the slope of the free energy curve. (*E*) The number of FtsZ molecules, however, remains relatively constant during contraction. (*F*) The number of lateral contacts between FtsZ increases during contraction while the number of polymer bonds remains relatively constant. (*G*) We compute the contraction force as a function of the lateral interaction energy (symbols), which agrees with the prediction of van der Waals model of Eq. **1** (solid line).

action of PBP3 and peptidoglycan synthesis proteins that modify the cell wall (8). In our simulation, we allow the radius of the mid-cell to vary and compute the acceptance of radius change using the Metropolis criterion. Results unambiguously show that the FtsZ density increase is achieved by decreasing the cell radius, and the number of FtsZ monomers in the ring is nearly constant (Fig. 2). FtsZ density increases by Z-ring contraction, not by recruiting more FtsZ monomers.

We compute the Z-ring free energy as a function of ring radius and lateral contact energy. Fig. 2 shows the computed Z-ring free energy, which decreases linearly from a cell radius of 500 nm to 250 nm. The percentage of FtsZ occupancy in the low MinC mid-cell region increases from ≈30% to ≈60%. The contractile force, which is the slope of the free energy versus radius, shows a proportional relationship with the lateral contact energy, increasing linearly from 5 pN at $e_2 = -1.0\ k_BT$ to 20 pN at $e_2 = -4\ k_BT$. These forces are consistent with estimated values for accomplishing cytokinesis in *E. coli* (8). For *Bacillus subtillis*, the cell wall is stiffer, and a larger contractile force is needed (8). Computation shows that 50 pN of force can be achieved by lowering e_2 further to $-9\ k_BT$, which is still

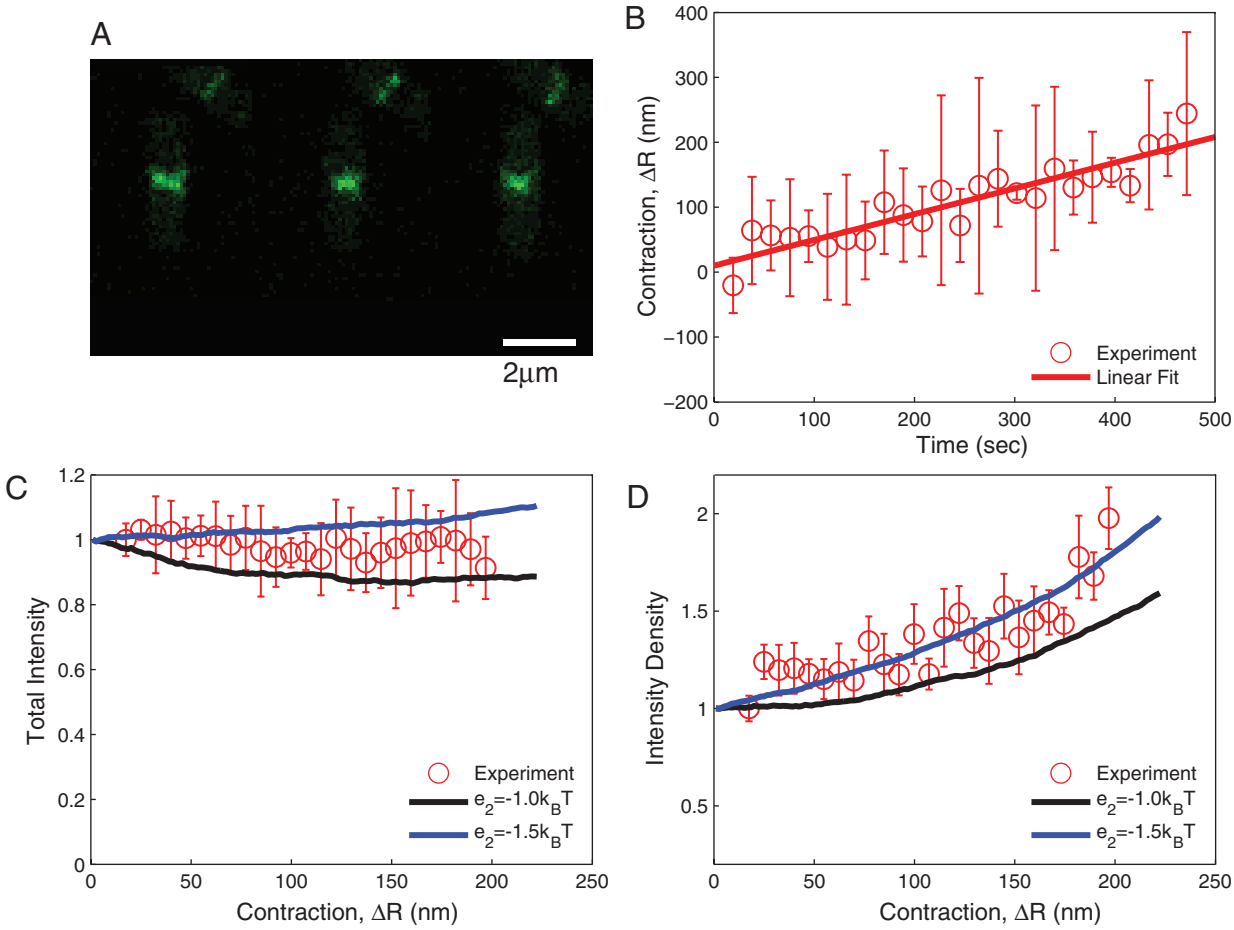

Fig. 3. We use fluorescence images of dividing bacterial cells to verify model predictions. (*A*) Images of dividing *E. coli* with FtsZ::GFP. (*B*) The ring radius decreases during division. (*C*) The measured total fluorescence intensity (symbols) of the ring remains constant, suggesting that the total number of FtsZ in the ring is constant during division. (*D*) The measured fluorescent intensity density (symbols), or the FtsZ density is increasing, reminiscent of Fig. 2*C*. The solid lines in *C* and *D* are computed results from our model. The data suggest that e_2 is between −1.0 and −1.5 k_BT.

significantly smaller than e_1. To show that lateral interactions between FtsZ filaments drive contraction, Fig. 2*F* shows that the number of lateral bonds is increasing during contraction. The number of polymer bonds, however, is constant. Together, these results show that the contractile force in the Z-ring results from a thermodynamic transition that increases FtsZ density: condensation of FtsZ filaments can drive bacterial cytokinesis.

Microscopy Results. To further validate our FtsZ condensation model, we measured the fluorescence intensity of FtsZ::GFP during *E. coli* division (Fig. 3). The measured total number of FtsZ in the Z-ring was essentially constant. The measured change in fluorescence intensity density, which reflects the change in the number of FtsZ per unit area in the ring, increased, in agreement with the predictions of the model. This observed condensation suggests that the lateral interaction is weak, $e_2 \approx -1.0$ to $-1.5\ k_BT$. The measured fluorescence intensities during division are consistent with our model predictions.

Overexpression of FtsZ and FtsA. Failure of division is often observed when the expression levels of FtsZ and FtsA are perturbed (16, 24). Overexpression of FtsZ causes a spiral like FtsZ macrostructure connected to the ring (25). Our model shows that these phenotypes arise from perturbed initial ring formation. When there is excess FtsZ in the cytoplasm, the density of FtsZ in the ring increases as well. When we increase the number of FtsZ in the cell from 10,000 to 40,000, the percentage of occupancy at mid-cell region increases from 30% to 90%: The ring is too dense and cannot increase its density further; cell division is blocked (Fig. 4*F*). Furthermore, when the FtsZ expression level is too high, filaments in the mid-cell region become significantly longer than the wild-type cell. A large fraction of FtsZ filaments are also not anchored to the membrane. When combined with repulsive interactions with the nucleoid (26), dynamic spiral-like FtsZ structures develop. Our model also similarly explains why excess FtsA inhibits cytokinesis (Fig. 4*E*, *SI Text*). Excess FtsA recruits too many FtsZ to the ring and the ring density is also too high to undergo contraction. Inhibiting GTP hydrolysis, however, slows down monomer turnover. This does not stop ring contraction, but contraction speed slows considerably.

van der Waals' Picture of Z-ring Condensation. The emerging picture of FtsZ condensation during division is reminiscent of the gas-liquid phase transition phenomena in attractive fluids, and can be simply explained with the classic model of van der Waals (27). The free energy of the Z-ring can be approximately written as:

$$F = \int d\mathbf{r} k_B T \rho \ln \frac{b\rho}{1-b\rho} + \frac{1}{2}\int d\mathbf{r} \int d\mathbf{r}' \rho(\mathbf{r}) u(\mathbf{r}, \mathbf{r}') \rho(\mathbf{r}') - \int d\mathbf{r} \mu(\mathbf{r}) \rho(\mathbf{r}) \quad [1]$$

where ρ is the FtsZ particle density, $u(\mathbf{r},\mathbf{r}')$ is the attractive interaction energy between particles and μ is the chemical poten-

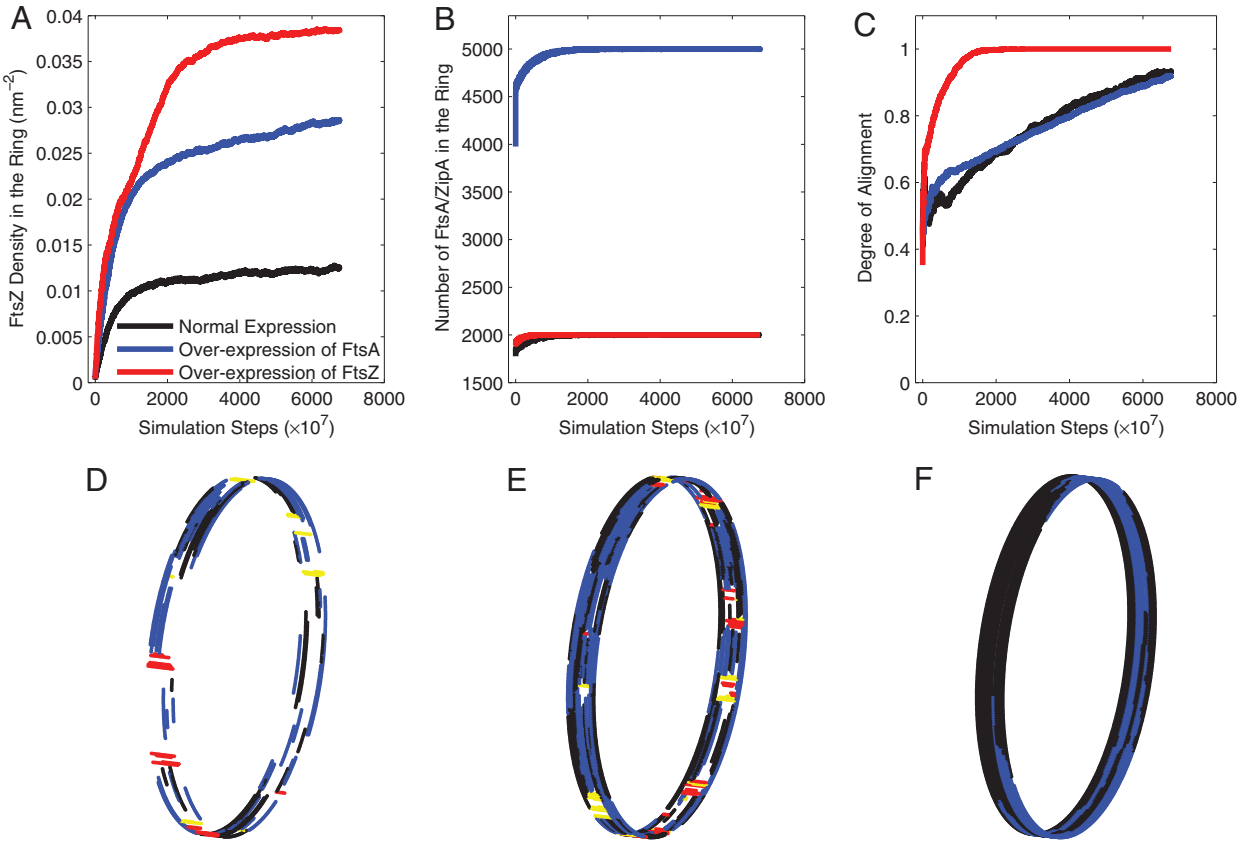

Fig. 4. Overexpression of either FtsZ or FtsA stops division. The model shows that the density of FtsZ in the ring is elevated when there is excess FtsZ or FtsA, further density increase is not possible, thus preventing condensation. (*A*) The density of FtsZ in the ring is significantly higher. (*B*) Excess FtsA+ZipA is recruited to the ring when there is overexpression of FtsA/ZipA. (*C*) The degree of alignment of FtsZ filaments higher when there is overexpression of FtsZ. (*D–F*) Model snap-shots of the Z-ring, showing normal levels of FtsZ and FtsA (*D*), overexpression of FtsA (*E*), and overexpressions of FtsZ (*F*).

tial. The first term accounts for the entropy of FtsZ particles and the effect of molecular size, where b is a molecular volume (size of our lattice). The second term describes FtsZ–FtsZ attraction, which has longitudinal and lateral contributions. The third term is the chemical potential term, which also includes favorable interaction with FtsA/ZipA. In our model, FtsZ filaments can interact in two ways. Therefore, we can write the second term as $e_1n_1 + e_2n_2$, where n_1 is the number of polymer bonds and n_2 is the number of lateral bonds. This estimate shows that the system achieves minimum free energy when all filaments orient in the hoop direction. Z-ring contraction is, however, different from the usual liquid-gas transition where instead of increasing density by changing the chemical potential, the density increase is achieved by increasing the lateral attraction between FtsZ filaments. The contractile force can be estimated by taking the derivative of the free energy with respect to the radius. The comparison between van der Waals theory and simulations is shown in Fig. 2*G*.

Role of GTP Hydrolysis. GTP hydrolysis is not explicitly modeled in the present work. The Monte Carlo move of breaking a FtsZ polymer bond contains the GTP hydrolysis step. We have pointed out in a separate publication that GTP hydrolysis increases the rate of polymer bond breakage (13). Thus, GTP hydrolysis increases the rate of monomer turnover in the polymer and facilitates the gradual morphological change of the Z-ring. A FtsZ mutant, FtsZ2, has been shown to have dramatically reduced GTP hydrolysis activity. Yet, the cells with FtsZ2 still divide, although the cells display an elongated morphology (6, 28). Our model indicates that if GTP hydrolysis is removed, the monomer turnover slows. The division force is similar, but the contraction would be significantly slower. Therefore, the cell wall grows more in the axial direction than the radial direction, leading to elongated cells.

Incomplete Z-rings Also Facilitate Division. Fig. 2*D* shows that the force is relatively constant function of the ring radius. Indeed, in our model, contraction is also observed when the filaments do not form a complete ring. An arc of FtsZ filaments also contracts using the same mechanism. The contraction force is a linear function of the size of the arc and can be predicted from the free energy expression of Eq. **1**. Cells with incomplete Z-rings have been observed to form invaginations (29). Our model suggests that the mechanism is the same as the full ring: Contraction from an incomplete ring generates an inward force that directs cell wall growth.

Discussion

Our model provides a molecular explanation of bacterial division and proposes a mechanism of biological force generation. The model shows that a microscale phase transition driven by molecular attraction between FtsZ filaments can generate contractile forces of 8–50 pN. Cell-wall growth and remodeling, under the influence of the contractile force, generate the division septum. Recent in vitro reconstitution of FtsZ in vesicles has shown that FtsZ generate a weak contractile force without other proteins, consistent with our model predictions (7).

When studying FtsZ filament in vitro, Erickson *et al.* noticed that GDP-FtsZ filaments adopt a highly curved structure whereas GTP-FtsZ is relatively straight (9). The structural basis of this curvature change was also discussed (30). Thus, GTP hydrolysis seems to induce a conformational change in FtsZ filaments. Because FtsZ-filaments have mechanical rigidity, the curvature

change can generate a mechanical force. The rigidity of FtsZ filaments have been estimated, and the persistence length, l_p, of FtsZ filaments is ≈180 nm, which is much smaller than F-actin (12). The mechanical energy of a single filament is then

$$E = \frac{1}{2} L l_p k_B T (\kappa - \kappa_0)^2 \quad [2]$$

where L is the length of the filament, κ_0 is the preferred curvature, and κ is the instantaneous curvature. During contraction, $\kappa = 1/R$, where R is the radius of the cell. κ_0 for GTP-FtsZ is 0 (straight), and $\kappa_0 = (10\ \text{nm})^{-1} = 0.1$ for GDP-FtsZ (9). Assuming that all monomers in the filaments simultaneously convert to GDP, then the total energy of the ring is

$$F = n \frac{1}{2} \langle L \rangle l_p k_B T \left[\frac{1}{R} - 0.1 \right]^2 \quad [3]$$

where n is the average number of FtsZ filaments and $\langle L \rangle$ is the average length. The force is then

$$f = n \langle L \rangle l_p k_B T \left[\frac{1}{R} - 0.1 \right] \frac{1}{R^2} \quad [4]$$

From our model, we estimate that $n \approx 90$, and $\langle L \rangle \approx 120$ nm. Thus, the force at the initial radius of $R = 500$ nm is at most 2.8 pN. This is small when compared with the forces generated from condensation. Considering that the filaments are generally disordered and are not always aligned and that GTP hydrolysis in the Z-ring is probably not a concerted process, the result is an overestimate. A recent model based on this curvature change mechanism from GTP hydrolysis to estimate the Z-ring force has been proposed (31). However, they used a significantly stiffer filament (l_p = 14,000–17,000 nm) than what is observed. Actual FtsZ polymers are 100 times softer. Therefore, the GTP hydrolysis-associated conformational change is probably not the force generation mechanism. FtsZ filaments are too soft to generate contractile forces using conformational changes.

Note that the contractile force can exist before the actual observed contraction. However, the force is too small (5–50 pN) to make any appreciable mechanical deformations (8). Only when the wall synthesis proteins (PBP) are active and the Z-ring is anchored to the cell wall can the contractile force influence the progress of the new cell wall. The timing and speed of division must coincide with the activity of PBP proteins.

Because polymer bonds competes with the entropy of dissociating into the cytoplasm, monomers continuous exchange with the environment in a dynamic manner. The exchange is the catalyzed by GTP hydrolysis, which serves to break polymer bonds (13). Therefore, the role of GTP is to facilitate monomer exchange and reorganization of the Z-ring. However, GTP hydrolysis of FtsZ is not critical for cytokinesis. GTP hydrolysis is not the direct energy source of contraction. Other proteins recruited to the ring, which change the lateral interaction between FtsZ, contribute to the condensation and force generation. By modulating the local environment of the ring, one can obtain a variety of contractile forces.

A surprising aspect of our finding is that a sometimes discontinuous ring can generate contractile force. Indeed, there are significant voids and empty space in the initial low-density Z-ring. However, the filaments elongate and shorten continuously (facilitated by bond formation and fragmentation), and the thermodynamic force is the result of averaging over many instantaneous configurations. During division, because the cell wall is growing inward (under the influence of the contractile force), the wall also does not expand when the ring is disconnected. On the time scale of cell wall growth, the ring fluctuates between many configurations. Thus, the average thermodynamic force is the quantity that drives the growth of the cell wall and ring contraction. Therefore, the model is an example of collective force generation completely independent of motor activities. There are many components in biological systems that interact with each other; therefore, similar thermodynamic forces must exist. Our model is a general mechanism that should be applicable in other settings.

SI. Further information, including Figs. S1–S8 and Tables S1 and S2, is available in the supporting information.

1. Bi EF, Lutkenhaus J (1991) FtsZ ring structure associated with division in Escherichia coli. *Nature* 354:161–164.
2. Bramhill D (1997) Bacterial cell division. *Annu Rev Cell* Dev Biol 13:395–424.
3. Lowe J, van den Ent F, Amos LA (2004) Molecules of the bacterial cytoskeleton. *Annu Rev Biophys Biomol Struct* 33:177–198.
4. Erickson HP (1995) FtsZ, a prokaryotic homolog of tubulin. *Cell* 80:367–370.
5. de Boer P, Crossley R, Rothfield L (1992) The essential bacterial cell-division protein FtsZ is a GTPase. *Nature* 359:254–256.
6. Mukherjee A, Saez C, Lutkenhaus J (2001) Assembly of an FtsZ mutant deficient in GTPase activity has implications for FtsZ assembly and the role of the Z ring in cell division. *J Bacteriol* 183:7190–7197.
7. Osawa M, Anderson DE, Erickson HP (2008) Reconstitution of contractile FtsZ rings in liposomes. *Science* 320:792–794.
8. Lan G, Wolgemuth CW, Sun SX (2007) Z-ring force and cell shape during division in rod-like bacteria. *Proc Natl Acad Sci USA* 104:16110–16115.
9. Erickson HP, Taylor DW, Taylor KA, Bramhill D (1996) Bacterial cell division protein FtsZ assembles into protofilament sheets and minirings, structural homologs of tubulin polymers. *Proc Natl Acad Sci USA* 93:519–523.
10. Mukherjee A, Lutkenhaus J (1999) Analysis of FtsZ Assembly by light scattering and determination of the role of divalent metal cations. *J Bacteriol* 181:823–832.
11. Lowe J, Amos JA (1999) Tubulin-like protofilaments in Ca^{2+}-induced FtsZ sheets. *EMBO J* 18:2364–2371.
12. Dajkovic A, Lan G, Sun SX, Wirtz D, Lutkenhaus J (2008) MinC spatially controls bacterial cytokinesis by antagonizing the scaffolding function of FtsZ. *Curr Biol* 18:235–244.
13. Lan G, Dajkovic A, Wirtz D, Sun SX (2008) Polymerization and bundling kinetics of FtsZ filaments. *Biophys J* 95:4045–4056.
14. Chen Y, Erickson HP (2005) Rapid in vitro assembly dynamics and subunit turnover of FtsZ demonstrated by fluorescence resonance energy transfer. *J Biol Chem* 280:22549–22554.
15. Lutkenhaus J (2007) Assembly dynamics of the bacterial MinCDE system and spatial regulation of the Z ring. *Annu Rev Biochem* 76:539–562.
16. Hale AC, de Boer PAJ (1997) Direct binding of FtsZ to ZipA, an essential component of the septal ring structure that mediates cell division in E. coli. *Cell* 88:175–185.
17. Hale AC, Rhee AC, de Boer PAJ (2000) ZipA-Induced bundling of FtsZ polymers mediated by an interaction between C-terminal domains. *J Bacteriol* 182:5153–5166.
18. RayChaudhuri D (1999) ZipA is a MAP-Tau homolog and is essential for structural integrity of the cytokinetic FtsZ ring during bacterial cell division. *EMBO J* 18:2372–2383.
19. Pichoff S, Lutkenhaus J (2002) Unique and overlapping roles for ZipA and FtsA in septal ring assembly in Escherichia coli. *EMBO J* 21:685–693.
20. Margolin W (2004) *Molecules in Time and Space: Bacterial Shape, Division and Phylogeny* (Springer, Berlin).
21. Stricker J, Maddox P, Salmon ED, Erickson HP (2002) Rapid assembly dynamics of the Escherichia coli FtsZ-ring demonstrated by fluorescence recovery after photobleaching. *Proc Natl Acad Sci USA* 99:3171–3175.
22. Rueda S, Vicente M, Mingorance J (2003) Concentration and assembly of the division ring proteins FtsZ, FtsA, and ZipA during the Escherichia coli cell cycle. *J Bacteriol* 185:3344–3351.
23. Li Z, Trimble MJ, Brun YV, Jensen GJ (2007) The structure of FtsZ filaments in vivo suggests a force-generating role in cell division. *EMBO J* 26:4694–4708.
24. Dai K, Lutkenhaus J (1992) The proper ratio of FtsZ to FtsA is required for cell division to occur in Escherichia coli. *J Bacteriol* 174:6145–6151.
25. Ma X, Ehrhardt DW, Margolin W (1996) Colocalization of cell division proteins FtsZ and FtsA to cytoskeletal structures in living Escherichia coli cells by using green fluorescent protein. *Proc Natl Acad Sci USA* 93:12998–13003.
26. Sun Q, Margolin W (2001) Influence of the nucleoid on placement of FtsZ and MinE rings in Escherichia coli. *J Bacteriol* 183:1413–1422.
27. Rowlinson JS, Widom B (1982) *Molecular Theory of Capillarity*. (Dover, Mineaola, NY).
28. Dai K, Mukherjee A, Xu Y, Lutkenhaus J (1994) Mutation in ftsZ that confer resistance to SulA affect the interaction of FtsZ with GTP. *J Bacteriol* 176:130–136.
29. Addinall SG, Lutkenhaus J (1996) FtsZ-spirals and -arcs determine the shape of the invaginating septa in some mutants of Escherichia coli. *Mol Microbiol* 22:231–237.
30. Olivia MA, Trambaiolo D, Lowe J (2007) Structural insights into the conformational variability of FtsZ. *J Mol Biol*, 373:1229–1242.
31. Ghosh B, Sain (2008) A Origin of contractile force during cell division of bacteria. *Phys Rev Lett*, 101:178101.